JOURNAL OF GUIDANCE, CONTROL, AND DYNAMICS
Vol. 34, No. 1, January–February 2011

Merging of Air Traffic Flows

Andre Michelin,* Moshe Idan,† and Jason L. Speyer‡
University of California, Los Angeles, Los Angeles, California 90095-1597

DOI: 10.2514/1.51134

The problem of merging two or more flows of aircraft in a horizontal plane is considered. The aircraft aim to reach a target flow with the minimal amount of turning, while maintaining a given separation between them. Neither a priori sequencing nor scheduling of the merging aircraft is assumed. The individual trajectories for each aircraft are computed using optimization, and a subset of these optimal trajectories serve as a basis for merging multiple aircraft. A second optimization step produces trajectories for each aircraft to ensure both effective merging into the flow and sufficient separation. This generates the sequencing of the merging aircraft. Simulations of several merging scenarios illustrate the approach and show its results. A statistical study of the influence of the problem parameters on the success of the merging algorithm provides a guideline for the design of the airspace around the merging area. The proposed algorithm can be used for automatic en route and terminal area merging tasks within future more automated air traffic control systems.

I. Introduction

THE primary objectives of air traffic control are to prevent collisions between aircraft (A/C) and organize flows of traffic. Studies have predicted that during the next two decades, demand will increase significantly and that the current air traffic control system will not sustain this amount of traffic [1,2]. A mandate for the design and deployment of an air transportation system to meet the nation's needs in 2025 was established in 2003. This new system, called NextGen[§] (Next Generation Air Transportation System) will have to be, among other things, capable of providing two to three times the current air vehicle operations. Assistance to the controllers will be required for them to support this increase in traffic while maintaining a reasonable controller workload. This can be provided by automation of specific tasks and by a greater automation of the system as a whole. Currently, airplanes follow fixed airways, for simplicity and ease of work for controllers. But as the traffic increases, the capacity limits of those airways will be reached, leading to unacceptable traffic delays. NextGen includes as an objective the implementation of the free-flight paradigm, which would allow for better use of the available airspace. The free-flight concept requires addressing a number of open issues, such as trajectory synthesis for the aircraft to comply with their destination and trajectory requirement while satisfying overall aerospace constraints (minimum separation, time constraints, etc.). In particular, merging flows of aircraft requires great attention from the controllers. Automating this task would be of great interest.

The goal of this work is to derive an algorithm for automatic merging of multiple aircraft into a given flow. The aircraft are required to merge into a target flow, which can be a preferred physical flow or a virtual path. The integral of the absolute value of the turn rate along the trajectory was chosen as the cost to minimize. So, each A/C aims to reach the target flow with the minimal amount of turning, while maintaining a given separation with the other A/C. Although one could address 3-D merging, in this study the merging is assumed to be planar, constrained to the horizontal plane.

In a previous effort to provide a tool to assist controllers in the terminal areas (TRACON), the Final Approach Spacing Tool (FAST [3]) was developed at NASA Ames Research Center. FAST provided landing sequences and landing runway assignments using a fuzzy-reasoning-based algorithm for sequencing arriving air traffic [4]. It performed trajectory-based planning by breaking the whole sequencing problem into smaller decisions. The sequencing and conflict resolution were performed serially: only once the sequencing and trajectory synthesis for the chosen aircraft sequence were completed was each aircraft deconflicted with the aircraft sequence ahead of it on each flight segment. This paradigm has exhibited some significant negative side-effects, such as reliance on derived criteria (e.g., delay incurred) rather than trajectory-based criteria (e.g., time to merge), thereby ineffectively handling certain typical merging scenarios [5]. Concurrent sequencing and deconfliction was attempted [5] to circumvent these limitations. A heuristic algorithm based on the discrete representation of the 4-D trajectories was developed but never implemented, as it was predicted the increase in controller workload would be unacceptable.

Work on minimal-time horizontal guidance of aircraft has been reported in the past: e.g., by Erzberger and Lee [6], Pecsvaradi [7], and Bolender and Slater [8]. Only a single aircraft merging to a line or to a given point (intercept problem) was considered, thus no separation constraints were considered. Also, merging to a particular point is useful to the problem at hand only once the sequencing of the A/C, as well as the slots assigned to each A/C, have been determined. These problems are not straightforward, and the methodology proposed in this paper bypasses this step. Studies have shown that the most significant part of National Airspace System delays (approximately 70%) are due to weather [9]. Thus optimizing with respect to time will only marginally reduce the delays and is therefore not necessarily a valid goal in practice. In [10] a linear programming approach for conflict resolution in air traffic problems is used, with application to a merging scenario. However, trajectories are discretized, and nonlinear functions are approximated linearly. In this work a unified traffic merging approach that tries to circumvent those difficulties is proposed.

This paper is organized as follows: In Sec. II the merging problem for a single A/C is solved; i.e., the minimum-turn merging trajectory (or trajectories) when no separation constraints exist is determined. This is done by solving an optimal control problem with two boundary constraints (initial and final states). Constant velocities and bounded turn rates are assumed. Unlike the minimum-time paradigm, the use of the total amount of turning as a cost function provides solutions with an attractive property: namely, that for a large

Received 11 June 2010; revision received 27 August 2010; accepted for publication 28 August 2010.

*Research Assistant, Department of Mechanical and Aerospace Engineering; amichelin@ucla.edu.

†Associate Professor, Aerospace Engineering, Technion—Israel Institute of Technology; oshe.idan@technion.ac.il.

‡Professor, Department of Mechanical and Aerospace Engineering; peyer@seas.ucla.edu.

§Data available online at http://www.ncat.com/ngats and http://www.faa.gov/about/initiatives/nextgen [retrieved June 2010].

set of initial conditions, there are an infinite number of optimal trajectories. This fact is exploited in Sec. III, where the search for a conflict-free multi-aircraft merging solution is limited to a subset of these unconstrained optimal trajectories. The solution to the merge is the result of an optimization step performed by simulated annealing [11]. Results illustrating the capabilities of the algorithm are presented in Sec. IV. Finally, a statistical study relating the feasibility of safe merging with the parameters characterizing the merging zone is conducted in Sec. V. Concluding remarks are presented in Sec. VI.

II. Single A/C Merging into Flow with Bounds on Entry Point

A. Problem Formulation

As a first step in constructing a merging algorithm for multiple aircraft, the optimal merging of a single aircraft is studied. The resulting trajectory for a single A/C will serve as a primitive for the multiple A/C case. In this study it is assumed that each aircraft aims to reach the target flow with minimum amount of turning along the trajectory, the motivation being one of ease for the pilot, as well as comfort for passengers. In practice, upper and lower bounds on the merging point of an A/C in the flow are desirable. For example, a controller will usually require an A/C to be in the final approach path for landing before a certain fix. This leads to the following optimal control problem.

The simplified mass-point model is considered, and the trajectories are assumed to be 2-D planar. The state $z \in \mathbb{R}^3$ is defined to include the (x, y) position coordinates and the heading angle θ. The control is the turn rate of the aircraft, denoted u, which is assumed to be bounded as $u \in [u_{\min}, u_{\max}]$. The state dynamics are described by the differential equation:

$$\dot{z} = f(z,u,t) = \begin{cases} \dot{x} = v\cos(\theta) \\ \dot{y} = v\sin(\theta) \\ \dot{\theta} = u \end{cases} \qquad \text{with} \quad u_{\min} \le u \le u_{\max} \tag{1}$$

where v is the speed of the aircraft. In this study, v is assumed to be constant. Also, in practice, $u_{\min} = -u_{\max}$, which implies that the aircraft can turn in both directions with the same maximum turn rates.

The initial state $z(t_0) = \begin{bmatrix} x(t_0) & y(t_0) & \theta(t_0) \end{bmatrix}^T$ is assumed to be given. The target flow is assumed to be aligned with the y axis; i.e.,

$$x(t_f) = 0 \tag{2}$$

$$\theta(t_f) = \pi/2 \tag{3}$$

This is a nonlimiting assumption since the definition of the axes in the x–y plane is arbitrary. Upper and lower bounds on the merging point of an A/C in the flow are specified as

$$y(t_f) \in [y_{\min}, y_{\max}] \tag{4}$$

The cost to minimize is

$$J = \int_{t_0}^{t_f} |u| \, \mathrm{d}t \tag{5}$$

with terminal time t_f unspecified.

B. First-Order Necessary Conditions

The first-order necessary conditions for optimality are now derived using standard optimal control theory. The notation is similar to that of [12]. The general form of the cost is

$$J = \phi(z(t_f), t_f) + \int_{t_0}^{t_f} L(z,u,t) \, \mathrm{d}t \tag{6}$$

where ϕ is the terminal cost, which is a function of the terminal state and terminal time, and $L(z, u, t)$ is the Lagrangian. For the cost J defined in Eq. (5), the terminal cost ϕ is zero, and the Lagrangian is $L(z, u, t) = |u|$. The variational Hamiltonian is then defined as

$$H(z,u,t) = L(z,u,t) + \lambda^T f(z,u,t) = |u| + \lambda_1 v\cos(\theta) + \lambda_2 v\sin(\theta) + \lambda_3 u \tag{7}$$

where $\lambda \in \mathbb{R}^3$ is the vector of Lagrange multipliers associated with the dynamics constraints (1). Note that H defined in Eq. (7) is not an explicit function of time. Therefore, H remains constant along optimal paths. The terminal constraints on the state, given in Eqs. (2) and (3) are restated as

$$\psi_{\text{eq}}(z_{t_f}, t_f) = 0 \quad \text{with} \quad \psi_{\text{eq}}(z,t) = \begin{bmatrix} x \\ \theta - \pi/2 \end{bmatrix} \tag{8}$$

To be precise, the terminal constraint on θ is in fact modulo 2π and requires an extra bit of care. Again, Lagrange multipliers $\nu_{\text{eq}} = \begin{bmatrix} \nu_1 \\ \nu_3 \end{bmatrix} \in \mathbb{R}^2$ will be associated with the two terminal constraints described by Eq. (8). The interval constraint on $y(t_f)$ can be stated as

$$\psi_{\text{ineq}}(z_{t_f}, t_f) \le 0 \quad \text{with} \quad \psi_{\text{ineq}}(z,t) = \begin{bmatrix} y - y_{\max} \\ y_{\min} - y \end{bmatrix} \tag{9}$$

to which two additional Lagrange multipliers $\nu_{2_{\text{upp}}}$ and $\nu_{2_{\text{low}}}$ will be associated. Finally, the equality and inequality constraints are grouped into

$$\psi(z,t) = \begin{bmatrix} x \\ y - y_{\max} \\ y_{\min} - y \\ \theta - \pi/2 \end{bmatrix} \tag{10}$$

with the associated Lagrange multipliers $\nu = \begin{bmatrix} \nu_1 & \nu_{2_{\text{upp}}} & \nu_{2_{\text{low}}} \nu_3 \end{bmatrix}^T$.

The Pontryagin Maximum Principle [13] gives a set of necessary conditions that an optimal control solution u^* needs to satisfy. The adjoint variables (the Lagrange multipliers λ) are chosen to satisfy the differential equation

$$\dot{\lambda} = -\left(\frac{\partial H}{\partial z}\right)^T \tag{11}$$

with terminal value $\lambda(t_f)$ satisfying

$$\lambda(t_f)^T = \left(\frac{\partial \phi}{\partial z} + \nu^T \frac{\partial \psi}{\partial z}\right)_{t=t_f} \tag{12}$$

Then, the optimal control u^* has to minimize the Hamiltonian defined in Eq. (7):

$$u^* = \arg\min_u H \tag{13}$$

Although the Hamiltonian H is not differentiable in u, the minimization equation (13) is straightforward, since H, as a function of u, has one of the forms shown in Fig. 1, up to an additive constant that is not a function of u. It is only when $\lambda_3 = \pm 1$ that the minimizing value for u is not unique. Figure 1 shows the various possible generic shapes of the Hamiltonian as a function of u, for different values of λ_3. From this figure it is clear that u^* satisfying Eq. (13) will be

$$u^* = \begin{cases} u_{\min} & \text{if } \lambda_3 > 1 \\ 0 & \text{if } -1 < \lambda_3 < 1 \\ u_{\max} & \text{if } \lambda_3 < -1 \end{cases} \tag{14}$$

$$u^* \in [u_{\min}, 0] \quad \text{if } \lambda_3 = 1 \tag{15}$$

$$u^* \in [0, u_{\max}] \quad \text{if } \lambda_3 = -1 \tag{16}$$

Since t_f is unspecified, an additional necessary condition is

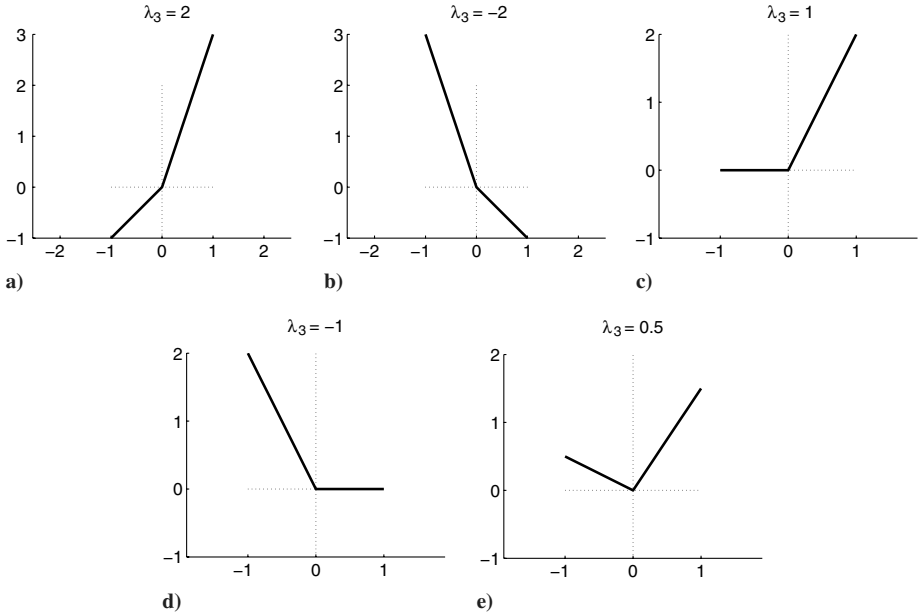

Fig. 1 Hamiltonian for different values of λ_3, with $u_{\min} = -1$ and $u_{\max} = 1$.

$$\left[\frac{\partial \phi}{\partial t} + \nu^T \frac{\partial \psi}{\partial t} + \left(\frac{\partial \phi}{\partial z} + \nu^T \frac{\partial \psi}{\partial z}\right) f + L\right]_{t=t_f} = 0 \tag{17}$$

Equation (17) is called the transversality condition and guarantees the optimality of the terminal time t_f (it implies that the solution is stationary with respect to t_f, while the terminal constraints are enforced). From Eq. (17) and the fact that the problem is stationary, the Hamiltonian equals zero along an optimal path.

Since in the present case $\phi = 0$ and

$$\frac{\partial \psi}{\partial z} = \begin{bmatrix} 1 & 0 & 0 \\ 0 & 1 & 0 \\ 0 & -1 & 0 \\ 0 & 0 & 1 \end{bmatrix}$$

Equations (11) and (12) become

$$\dot{\lambda}(t) = \begin{bmatrix} 0 \\ 0 \\ \lambda_1 \dot{y} - \lambda_2 \dot{x} \end{bmatrix} \tag{18}$$

$$\lambda(t_f) = \begin{bmatrix} \nu_1 \\ \nu_{2_{\text{upp}}} - \nu_{2_{\text{low}}} \\ \nu_3 \end{bmatrix} \tag{19}$$

For the inequality constraints (9), there are additional conditions on the associated multipliers:

$$\begin{cases} \psi_{\text{ineq}} \le 0 \\ \nu_{\text{ineq}} \ge 0 \\ \nu_{\text{ineq}}^T \psi_{\text{ineq}} = 0 \end{cases} \quad \text{with} \quad \nu_{\text{ineq}} = \begin{bmatrix} \nu_{2_{\text{upp}}} \\ \nu_{2_{\text{low}}} \end{bmatrix} \tag{20}$$

Equation (20) essentially states that the multipliers associated with inequality constraints are positive and equal to zero when the constraint is not active. In the present case, since both constraints cannot be active at the same time, at least one ν_2 is zero.

The free parameters in the above equations are ν_1, the quantity $\nu_{2_{\text{upp}}} - \nu_{2_{\text{low}}}$ or y_f (terminal value of y), depending on whether or not the terminal inequality constraints are active, ν_3 and t_f. These parameters are determined by the three boundary state conditions (either initial or terminal) and the transversality condition. The solution to the system of Eqs. (18) and (19) has a particular form: λ_3 is a *linear* function of x and y, since from Eq. (18), λ_1 and λ_2 are constants and

$$\lambda_3 = \lambda_1 y - \lambda_2 x + \text{const} \tag{21}$$

where const is an additive constant determined by the boundary conditions, and λ_1 and λ_2 are equal to ν_1 and $\nu_{2_{\text{upp}}} - \nu_{2_{\text{low}}}$, respectively. Therefore, λ_3 is given by

$$\lambda_3 = \nu_1 (y - y_f) - (\nu_{2_{\text{upp}}} - \nu_{2_{\text{low}}}) x + \nu_3 \tag{22}$$

Now the transversality condition becomes

$$0 = (\nu_{2_{\text{upp}}} - \nu_{2_{\text{low}}}) v + \nu_3 u_f + |u_f| \tag{23}$$

Two cases can occur. If $\nu_1 \neq 0$ and/or $\nu_{2_{\text{upp}}} - \nu_{2_{\text{low}}} \neq 0$, then λ_3 is an explicit function of x and y, so the optimal control switches when the state crosses the curves where $\lambda_3 = \pm 1$. The switch curves are two parallel lines in the x–y plane. Their respective equations are

$$S^{\max}\text{: } \nu_1 y - (\nu_{2_{\text{upp}}} - \nu_{2_{\text{low}}}) x + \nu_3 - \nu_1 y_f + 1 = 0 \tag{24}$$

$$S^{\min}\text{: } \nu_1 y - (\nu_{2_{\text{upp}}} - \nu_{2_{\text{low}}}) x + \nu_3 - \nu_1 y_f - 1 = 0 \tag{25}$$

Along $S^{\max}$, $\lambda_3 = -1$, and along $S^{\min}$, $\lambda_3 = +1$. When the A/C trajectory in the x–y plane crosses $S^{\max}$, u^* switches between $u_{\max}$ and 0, and when the A/C trajectory crosses $S^{\min}$, u^* switches between $u_{\min}$ and 0, with 0 being the control between these two lines. Therefore, the trajectories consist of a succession of turns in opposite directions and at extreme turn rate, with a straight segment between the turns.

If $\nu_1 = 0$ and $\nu_{2_{\text{upp}}} - \nu_{2_{\text{low}}} = 0$, from Eq. (21) it is clear that λ_3 is independent of x and y (and thereby of time) and is a constant equal to ν_3. Also, Eqs. (8), (14–16), and (23) imply that $|\nu_3| \le 1$. Therefore, there are two possible cases:

1) If $|\nu_3| < 1$, from Eq. (23) u^* will also be constant equal to 0, which only is a valid solution if z_0 is already in the flow;

2) If $|\nu_3| = 1$, then u^* can take any value in the interval $[0, u_{\max}]$ or $[u_{\min}, 0]$ (depending on the sign of ν_3) as long as the initial and terminal state boundaries are satisfied. This means that only turns in the same direction are allowed. This case leads to an infinite number of solutions, with an arbitrary number of turns at arbitrary turn rates. This phenomenon will be discussed further in the next subsection.

C. Characterization of Optimal Trajectories

First, the following remarks are made. The cost can be bounded from below as

$$J = \int_{t_0}^{t_f} |u| \, \mathrm{d}t \geq \left| \int_{t_0}^{t_f} u \, \mathrm{d}t \right| \tag{26}$$

Since $u = \dot{\theta}$,

$$J \geq \left| \int_{t_0}^{t_f} \dot{\theta} \, \mathrm{d}t \right| = |\theta(t_f) - \theta(t_0)| \tag{27}$$

This shows that since $\theta(t_f) = \pi/2, |\pi/2 - \theta_0|$ is a lower bound of the constrained optimization problem (a little care is required here due to the modulo 2π). Therefore, any path that has this value as a cost is globally optimal.

When $\nu_1 = 0$ and $\nu_{2_{upp}} - \nu_{2_{low}} = 0$, the transversality condition reduces to an inequality, and there can be an infinite number of optimal solutions. Indeed, the first-order necessary conditions lead to u^* taking values in an entire interval, and this is illustrated in Fig. 2. For the initial conditions depicted, all the paths have the same cost and are globally optimal, due to the previous remark.

1. *Candidate Strategies for Optimality*

The previous section gives the conditions that an optimal trajectory (if it exists) must satisfy. From these, all optimal paths are described. The previous discussion implies that there are essentially four possible control strategies that are candidates for optimality: $\mathbf{u}_R$ is only negative (including zero) turns (i.e., right turns and straight segments); $\mathbf{u}_L$ is only positive (including zero) turns (i.e., left turns and straight segments); $\mathbf{u}_{LSR}$ is an extreme left turn, a straight segment, and extreme right turn; and $\mathbf{u}_{RSL}$ is an extreme right turn, a straight segment, and extreme left turn.

Actually, other control strategies, consisting of more than two alternating turns, are also possible candidates. However, these trajectories will never be optimal. A proof by construction of this fact is given in Appendix A. Therefore, in the following discussion, the search for an optimal is limited to trajectories resulting from the four strategies given above.

For any given initial state, the cost for each of the four candidate strategies is derived, and the minimum is found. This will give the global optimum. By using the symmetry relative to the y axis of the problem, it can be concluded that symmetric initial conditions will have symmetric optimal solutions. So the space of initial states can be reduced. Two equivalent approaches are possible: either it is assumed, without loss of generality, that the initial point considered is in the left half of the x–y plane, and the heading can take any value, or it is assumed that the heading can only take values between $-\pi/2$ and $+\pi/2$, in which case the entire x–y plane needs to be considered. From now on, it will be assumed that $\theta_0 \in [-\pi/2, \pi/2]$ and the cost of each of the four strategies described above will be graphically determined all possible initial positions.

2. *Boundaries of Interest in the x–y Plane*

For a given θ_0, certain special lines and circles in the x–y plane are defined, that delimit regions of interest in the space of positions. It turns out that these lines are of significance in the problem at hand. Rather than explicit equations, graphs of these lines and circles for two different values of θ_0 are shown in Fig. 3, to give a sense of their structure. The equations are straightforward to find.

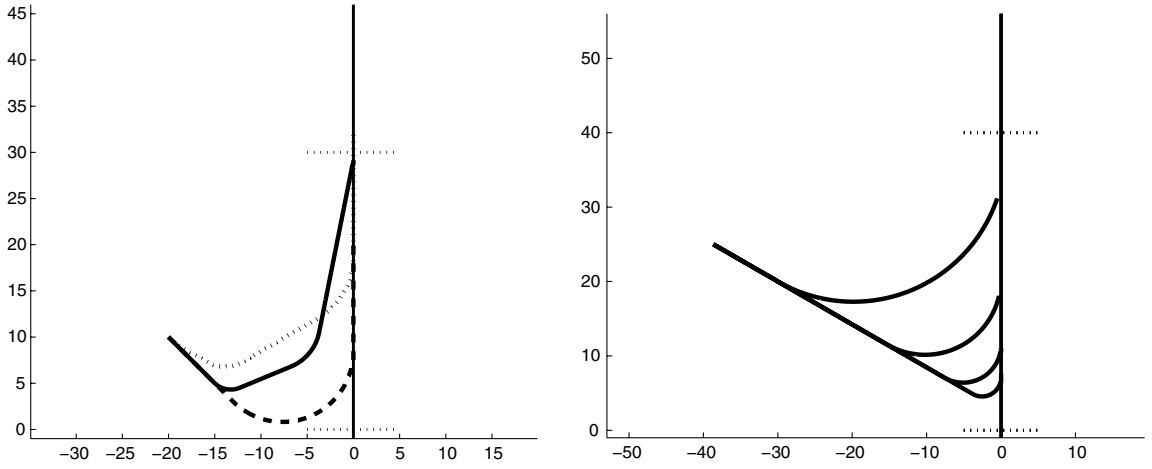

a) Global optima with 1 (dashes), 2 (dots), and 3 (solid) turns **b) Default path with different turn rates**

Fig. 2 Infinite character of the solution set.

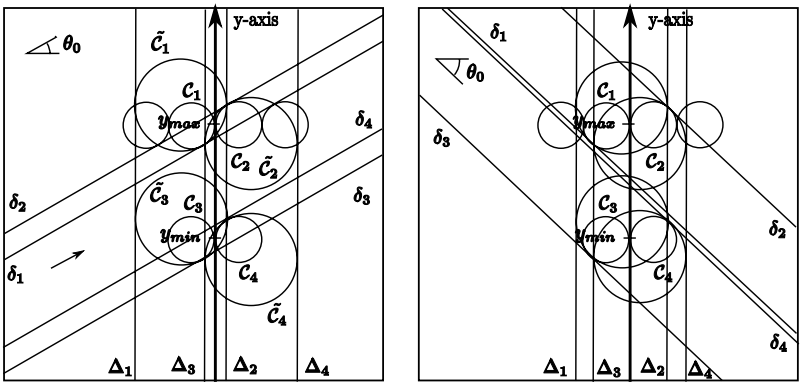

a) Regions of interest for initial heading of $\pi/6$ **b) Regions of interest for initial heading of $-\pi/4$**

Fig. 3 Regions of interest for different initial headings.

The circles $\mathcal{C}_1, \mathcal{C}_2, \mathcal{C}_3$, and $\mathcal{C}_4$ are circles of radius $r = v/u_{\max}$, with respective centers $(-r; y_{\max})$, $(r; y_{\max})$, $(-r; y_{\min})$, and $(r; y_{\min})$. The lines $\delta_1, \delta_2, \delta_3$, and δ_4 have a slope of $\tan(\theta_0)$ and are tangent to their respective circles $\mathcal{C}_i$. The large circles $\tilde{\mathcal{C}}_i$ have a radius of $2r$, are tangent to the lines δ_i at the same point as $\mathcal{C}_i$ and encircle $\mathcal{C}_i$. Finally, the lines Δ_1 and Δ_3 are vertical tangents to both $\tilde{\mathcal{C}}_1$ and $\tilde{\mathcal{C}}_3$, and the corresponding statement is true for the lines Δ_2 and Δ_4.

3. *Cost for Each Candidate Control Strategy*

For illustration purposes, a value for θ_0 is now picked, but the following discussion remains valid for all possible values of θ_0. The illustrations supporting the derivations are shown for $\theta_0 = \pi/6$. For this initial heading, the cost of each of the four strategies that are candidates for optimality is now determined, as a function of the initial position in the x–y plane. This is done graphically.

a. Only Left Turns. The regions of interest are depicted in Fig. 4a. If the initial position is in region A, then an acceptable merging can be performed by only turning left or going straight, with no loop necessary. However, if the initial point is not in region A, then it is impossible to reach the allowed merging interval without performing a full circle. Therefore, the cost is discontinuous at the boundaries of region A and jumps by an amount of 2π. So for this control strategy, the cost is $\pi/2 - \theta_0$ in region A and $2\pi + \pi/2 - \theta_0$ outside of region A.

b. Only Right Turns. The regions of interest are depicted in Fig. 4b. The cost is the same everywhere in the x–y plane. It has a constant value of $\pi + \theta_0 + \pi/2 = 3\pi/2 + \theta_0$.

c. Extreme Right Turn/Straight Segment/Extreme Left Turn. The regions of interest are depicted in Fig. 5a. Additional variables are defined to express the cost of such a strategy. The resulting trajectory is arcs of circles of radius $r = v/u_{\max}$, with a straight portion along a line tangential to both circles. The cost depends explicitly on the point of departure from the first circle. This is illustrated in Fig. 6.

The point N is such that $\mathbf{O_1N} \perp \mathbf{NM}$ and $\mathbf{NM}$ points toward the point M. This translates into

$$\cos(\theta_N - \theta_M) = \frac{r}{\|O_1M\|} \tag{28}$$

$$\cos(\theta_N - \pi/2 + \theta_M) > 0 \tag{29}$$

Equation (28) comes from $\langle \mathbf{O_1N}, \mathbf{NM} \rangle = 0$, and Eq. (29) comes from the fact that $\theta_N - \pi/2 + \theta_M$ is the angle between $\mathbf{O_1M}$ and $\mathbf{NM}$. Since these equations result in an angle modulo 2π, θ_N is defined to be in the interval $[\theta_0 + \pi/2 - 2\pi; \theta_0 + \pi/2)$.

The cost of this path from $(x_0; y_0; \theta_0)$ to $(0; y_f; \pi/2)$ is

$$J = (\theta_0 + \pi/2 - \theta_N) + (0 - (\theta_N - \pi)) \tag{30}$$

So

$$J = 3\pi/2 + \theta_0 - 2\theta_N \tag{31}$$

In this problem, the optimal terminal value y_f is not known and will depend on the initial state. It is determined graphically for simplicity. If the initial position is in region B, then $y_f \in [y_{\min}, y_{\max}]$, $\theta_N = \theta_0 + \pi/2$ (so no first turn) and the cost is

$$J_B = \pi/2 - \theta_0 \tag{32}$$

which is consistent with the cost derived for only left turns allowed. In region A and region C $y_f = y_{\max}$, and in region D $y_f = y_{\min}$. The costs have the expression of Eq. (31).

d. Extreme Left Turn/Straight Segment/Extreme Right Turn. The point N of departure from the first circle is characterized by the

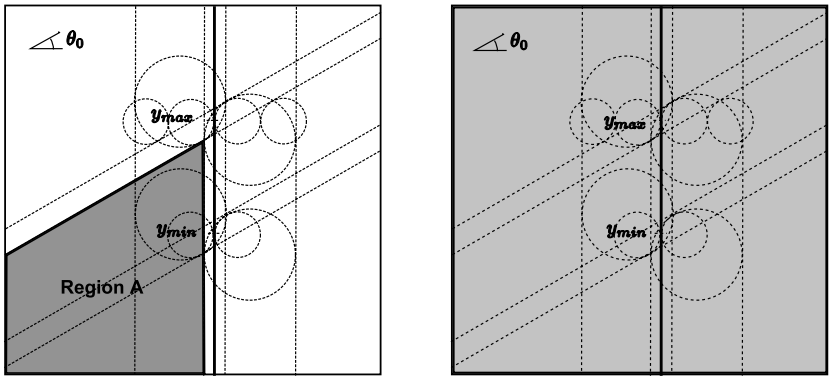

a) Optimal cost when only left turns allowed **b) Optimal cost when only right turns allowed**

Fig. 4 Optimal cost for trajectories with only one turn direction allowed.

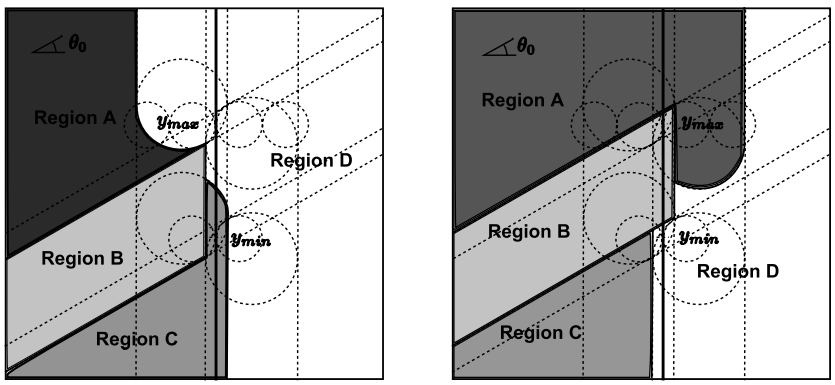

a) Optimal cost when right/straight/left **b) Optimal cost when left/straight/right**

Fig. 5 Optimal cost for S-shaped trajectories.

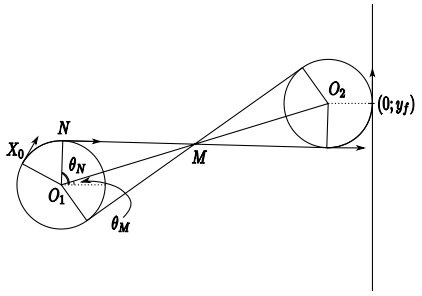

Fig. 6 Optimal right/straight/left path to a fixed point on target flow.

same equations (28) and (29), as shown in Fig. 7. Now the value of the solution θ_N to this system of equations in the interval $[\theta_0 - \pi/2; \theta_0 - \pi/2 + 2\pi)$ is determined, yielding the cost

$$J = \begin{cases} (\theta_N - (\theta_0 - \pi/2)) + (2\pi + \theta_N) & \text{if } \theta_N < 0 \\ (\theta_N - (\theta_0 - \pi/2)) + \theta_N & \text{if } \theta_N \geq 0 \end{cases} \tag{33}$$

or, equivalently,

$$J = \begin{cases} 2\theta_N - \theta_0 + 5\pi/2 & \text{if } \theta_N < 0 \\ 2\theta_N - \theta_0 + \pi/2 & \text{if } \theta_N \geq 0 \end{cases} \tag{34}$$

The regions of interest are depicted in Fig. 5b. If the initial position is in region B, then $y_f \in [y_{\min}, y_{\max}]$, $\theta_N = \theta_0 - \pi/2$ (so no first turn), and since $\theta_0 - \pi/2 < 0$, the cost is

$$J_B = \theta_0 + 3\pi/2 \tag{35}$$

which is consistent with the cost derived for only right turns allowed. In region A and region C $y_f = y_{\min}$, and in region D $y_f = y_{\max}$. The costs have the expression of Eq. (34).

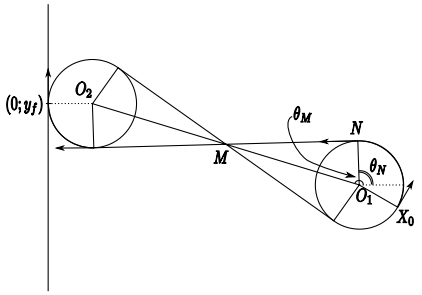

Fig. 7 Optimal left/straight/right path to a fixed point on target flow.

4. Overall Cost

The overall optimal strategy for any given initial state is the minimum between the four possible control strategies. One can proceed by successive minimizations to determine the optimal control in the different regions of the x–y plane. The costs of the four strategies discussed above are denoted J_1, J_2, J_3 and J_4, respectively, in the same order as presented. Since $-\pi/2 \leq \theta_0 < \pi/2$,

$$\pi/2 - \theta_0 \in [0; \pi] \tag{36}$$

$$5\pi/2 - \theta_0 \in [2\pi; 3\pi] \tag{37}$$

$$3\pi/2 + \theta_0 \in [\pi; 2\pi] \tag{38}$$

So

$$J_{12} \triangleq \min(J_1, J_2) = \begin{cases} J_1 & \text{if in region A of Fig. 4a} \\ J_2 & \text{elsewhere} \end{cases}$$

Now taking the third strategy into account, $J_3 = 3\pi/2 + \theta_0 - 2\theta_N$. Based on Fig. 5a, in region A $y_f = y_{\max}$, and $\theta_N > 0$, so $J_3 < J_2 = J_{12}$; in region B $J_3 = J_1 = J_{12}$; in region C $y_f = y_{\max}$ and $\theta_N < 0$, so $J_3 > J_2 \geq J_{12}$; and in region D $y_f = y_{\min}$ and $\theta_N < 0$, so $J_3 > J_2 \geq J_{12}$.

Therefore,

$$J_{123} \triangleq \min(J_1, J_2, J_3) = \begin{cases} J_1 & \text{if in region A of Fig. 4a} \\ J_3 & \text{if in region A of Fig. 5a} \\ J_2 & \text{elsewhere} \end{cases}$$

Finally, taking the last strategy into account,

$$J_4 = \begin{cases} 2\theta_N - \theta_0 + 5\pi/2 & \text{if } \theta_N < 0 \\ 2\theta_N - \theta_0 + \pi/2 & \text{if } \theta_N \geq 0 \end{cases}$$

Based on Fig. 5b, in region A $y_f = y_{\min}$ and $\theta_N \geq \pi$, so $J_4 = 2\theta_N - \theta_0 + \pi/2 \geq 5\pi/2 - \theta_0 > J_2 \geq J_{123}$; in region B $J_4 = J_2$; in region C $y_f = y_{\min}$ and $-\pi < \theta_N < 0$, so $J_4 = 2\theta_N - \theta_0 + 5\pi/2 J_2 > \pi/2 - \theta_0 = J_1 \geq J_{123}$; and in region D $y_f = y_{\max}$ and $0 \leq \theta_N \leq \pi$, so $J_4 = 2\theta_N - \theta_0 + \pi/2$. In this region, $J_{123} = J_2 = 3\pi/2 - \theta_0$, so $J_4 < J_{123}$ when $2\theta_N - \theta_0 + \pi/2 < 3\pi/2 - \theta_0$, which is equivalent to $\theta_N < \theta_0 + \pi/2$.

In conclusion,

$$J^* \triangleq \min(J_1, J_2, J_3, J_4)$$
$$= \begin{cases} J_1 & \text{if in region A of Fig. 4a} \\ J_3 & \text{if in region A of Fig. 5a} \\ J_4 & \text{elsewhere where } \theta_N < \theta_0 + \pi/2 \\ J_2 & \text{elsewhere where } \theta_N \geq \theta_0 + \pi/2 \end{cases}$$

This is illustrated in Fig. 8a. The cost value function for $\theta_0 = \pi/6$ is shown in Fig. 8b. It is discontinuous in x and y along certain boundaries. However, if the initial position is far enough from the y

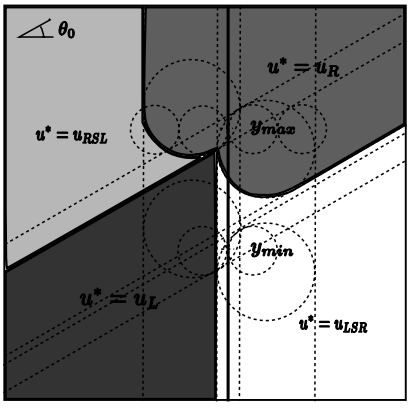

a) Optimal control strategies for $\theta_0 = \pi/6$

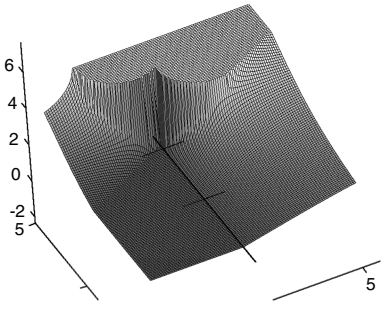

b) Optimal cost for $\theta_0 = \pi/6$

Fig. 8 Optimal control and cost when $\theta_0 = \pi/6$.

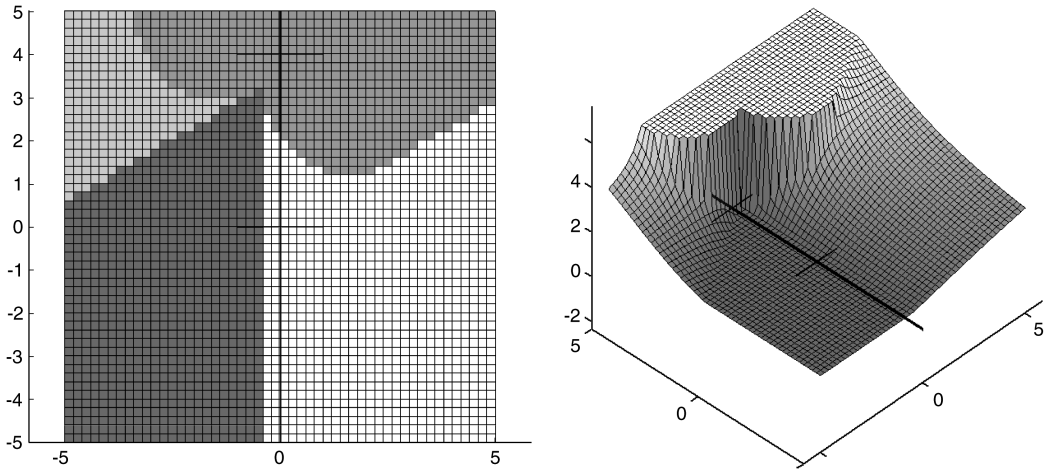

a) Regions for each strategy b) Optimal cost

Fig. 9 Optimal control and control when $\theta_0 = \pi/6$.

axis, then the cost is locally continuous in x and y, and the optimal control strategy can be determined a priori.

Figures 9–11 show the cost function and the regions corresponding to each of the four control strategies that are optimal for θ_0 equal to $\pi/6$, $-\pi/4$ and $5\pi/6$, respectively. As expected, the first and last graphs are symmetrical with respect to the y axis.

D. Conclusion and Remarks

The previous derivation allows one to define a priori regions in the state space for which the optimal cost and strategies are known and well-behaved functions. Initiating the merging procedure with aircraft constrained to these regions will allow for efficient merging solutions. When no bounds on the entry point are fixed, the structure of the candidate solutions are the same as in the previous section. However, for some initial conditions, no minimum will exist, only an infimum. If $\pi/2 \leq \theta_0 < 3\pi/2$, then, clearly, by turning at $u_{\min}$ until $\theta < \pi/2$, then going straight and then turning into the flow, the cost will be close to optimal (i.e., it will be arbitrarily close to $\theta_0 - \pi/2$), but due to the strict inequality, no minimum can be achieved. An illustration of this is given in Fig. 12.

As was shown above, for any initial condition, the set of minimum-turn solutions includes what is called a Dubins path [14] (so a turn–straight–turn path, or a degenerate form of such a path). When the terminal point is constrained, it was shown that the minimum-time path has this bang–off–bang structure [6,7,14,15], as does the minimum-turn solution. While in the minimum-turn case there are two parallel switch lines, in the minimum-time case there is only one switch line, and the straight portion of the solution is along the switch line (this occurrence is called a singular arc). So although the underlying structures are different, the resulting trajectories are the same in the two cases. Therefore, for a given initial point, the Dubins paths of the set of minimum-turn solutions also guarantee minimum time to their respective merging points. This additional information can be used in the decision making process. When the merging point is not fixed, the minimum-time solution is a unique Dubins path whose straight portion is always orthogonal to the target flow. The minimum-turn paradigm gives more flexibility by providing multiple optimal solutions. This property will be exploited when constructing the merging algorithm, presented in the next section.

III. Merging Multiple Aircraft

Multiple A/C are considered, all having the same dynamics described in the previous section, merging onto a target flow between two specified points on this flow. The initial state of each A/C is given and the configuration is assumed to be such that an optimal path exists for each individual A/C (cf. previous section). The minimum separation required between A/C, speeds and maximum turn rates are also given parameters. The setup includes also the definitions of the target flow assumed to be aligned with the y axis, together with the lower and upper bounds on the y axis delimiting the admissible region of entry into the flow.

Based on the conclusions of the previous section, if bounds on the entry points of the aircraft into the target flow are set, a minimum cost

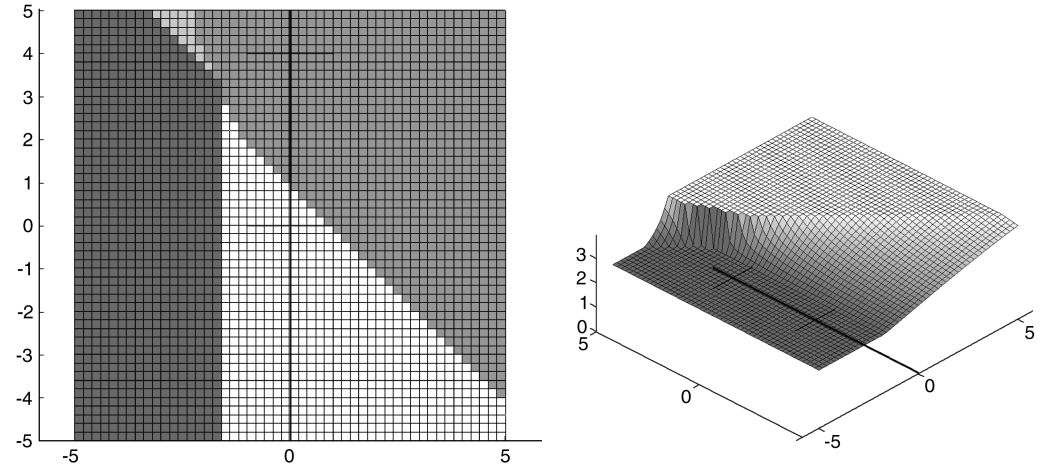

a) Regions for each strategy b) Optimal cost

Fig. 10 Optimal control and cost when $\theta_0 = -\pi/4$.

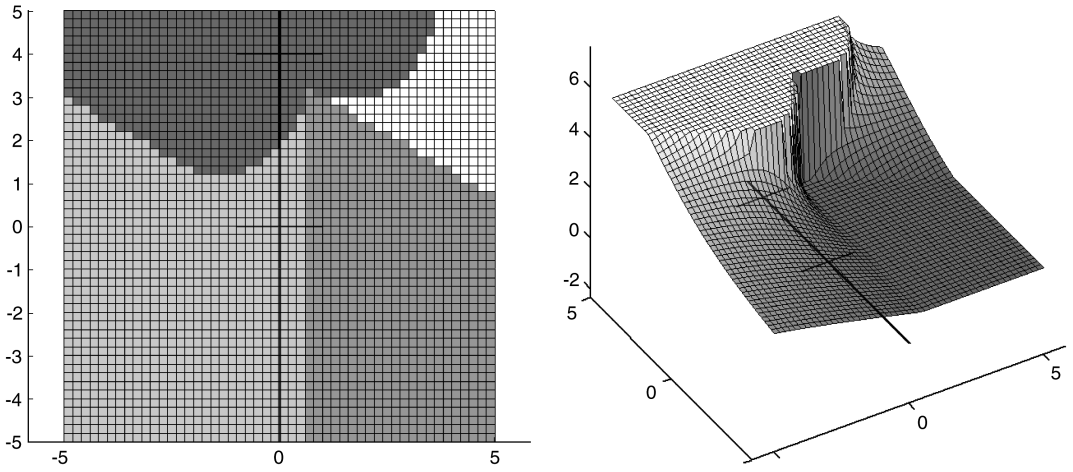

a) Regions for each strategy **b) Optimal cost**

Fig. 11 Optimal control and cost when $\theta_0 = 5\pi/6$.

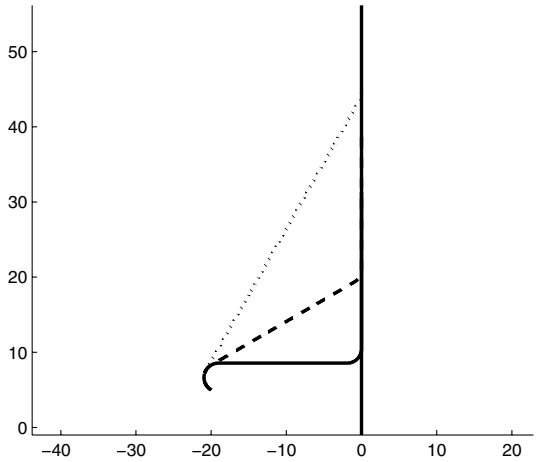

Fig. 12 If the initial heading is $\pi/2 \leq \theta_0 < 3\pi/2$, it is always possible, when no upper bound on y_f exists, to improve the cost to make it arbitrarily close to $\theta_0 - \pi/2$ (the cost is decreased from solid to dotted line).

path will always exist for any given A/C, but will not necessarily be unique. In fact, in this case, there may be infinitely many optimal paths. Although this is an advantage since it gives a certain degree of freedom while maintaining optimality, it makes a global optimization problem with multiple A/C challenging.

A. One-Parameter Trajectories

First, the search for solutions is limited to the set of trajectories composed of only two full rate turns with a straight portion between the two turns. Such a trajectory will be time-minimal to the chosen entry point. It will also be turn-optimal for all choices of entry point that require both turns to be in the same direction. For this subset of trajectories, the first turn entirely determines the evolution of the aircraft state for the duration of the merge. δ_i is defined such that $|\delta_i|$ is the duration of the first turn for aircraft A/C$_i$. δ_i can be positive or negative, with the following convention: if u_i is the control for A/C$_i$ during the first $|\delta_i|$ seconds, then

$$u_i = \text{sign}(\delta_i) u_{\max} \tag{39}$$

For a given δ_i, define

$$X_i(\delta_i) = \begin{bmatrix} x_i(t) \\ y_i(t) \\ \theta_i(t) \end{bmatrix}$$

for $t \in [0, T]$ (where T is the duration of the merge) to be the evolution of the state of A/C$_i$ when the control of A/C$_i$ is u_i given in (39) from $t = 0$ to $t = |\delta_i|$, then straight, until merging into the target flow at extreme turn rate. Also define the vector

$$\delta = [\, \delta_1 \quad \dots \quad \delta_N \,]^T$$

and the corresponding vector $X(\delta)$ of continuous time functions obtained from vertically concatenating the state trajectories of the N aircraft:

$$X(\delta) = \begin{bmatrix} X_1(\delta_1) \\ \vdots \\ X_N(\delta_N) \end{bmatrix} \in \mathcal{C}([0, T], \mathbb{R}^{3N})$$

Finally, the set of acceptable solutions is defined as the set of $\delta \in \mathbb{R}^N$ such that $X(\delta)$ is a valid merging solution and is denoted by Δ. Now define the functions:

$$h_i^+(X(\delta)) = y_{\min} - y_i(t_i^{\text{ent}})$$

and

$$h_i^-(X(\delta)) = y_i(t_i^{\text{ent}}) - y_{\max}$$

where t_i^{ent} is the time of first entry on the target flow for aircraft i not initially on the target flow, and

$$\sigma_{ij}(X(\delta)) = d_{ij} - \text{sep}_{\min}$$

where d_{ij} is the minimum distance between aircraft i and j during the merge, and $\text{sep}_{\min}$ is the minimum allowed separation. Functions h^+ and h^- will be used to force the aircraft to merge into the prescribed entry interval, while σ will be used to enforce the minimum separation between all pairs of aircraft during the merge. With these definitions,

$$\Delta = \{\delta \in \mathbb{R}^N | h_i^+(X(\delta)) \leq 0, \quad h_i^-(X(\delta)) \leq 0$$
$$\sigma_{ij}(X(\delta)) \leq 0, \quad \forall\ i, j = 1, \dots, N\}$$

or, equivalently,

$$\Delta = \{\delta \in \mathbb{R}^N | \max_{i,j} \max(h_i^+(X(\delta)), h_i^-(X(\delta)), \sigma_{ij}(X(\delta))) \leq 0\}$$

To solve the merging problem, one needs to find a δ in Δ. This is done by minimizing the cost function

$$C(\delta) = \max_{i,j} \max(h_i^+(X(\delta)), h_i^-(X(\delta)), \sigma_{ij}(X(\delta)))$$

using a simulated annealing search method [11]. The search is stopped as soon as the cost is negative. As a first guess, δ_{pref} is chosen

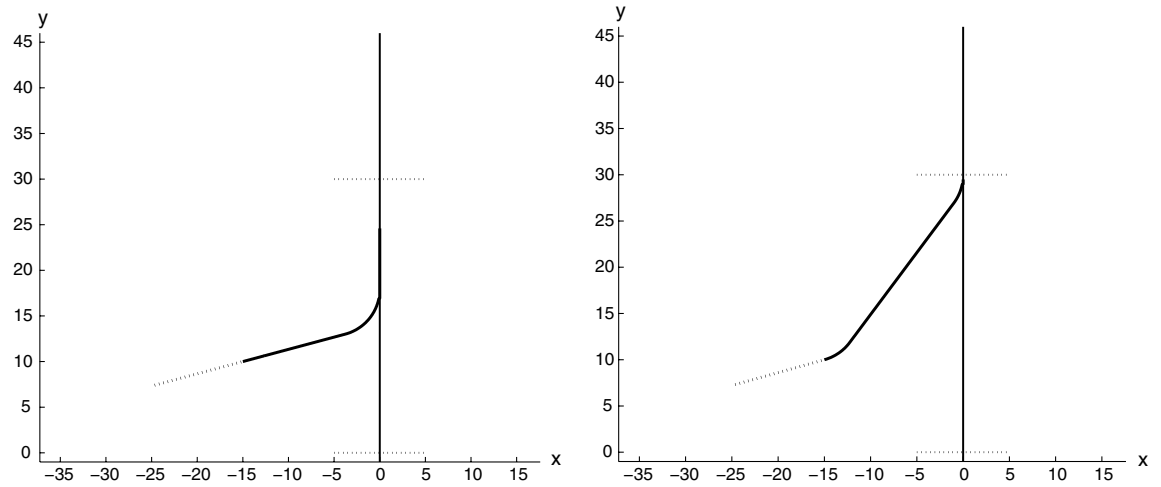

a) Minimum initial turn b) Minimum time

Fig. 13 Possible choices for default trajectories. The A/C are traveling along the dotted path, and the merging is initiated at the start of the full line.

that results in a *preferred (or default) trajectory*, which has desirable properties. If the cost for this δ_{pref} is negative, then the problem is solved by letting the aircraft follow these preferred trajectories, and the desired properties are obtained. These properties depend on the entry point of the aircraft on the target flow. For instance, if one chooses the entry point on the target flow that minimizes the first turn, then for A/C initially heading toward the allowed entry interval, the default trajectory will be to go straight as long as possible until the final turn into the flow, and therefore only require one turn, which could be desirable for workload concerns (fewer turns could translate into fewer controller commands). Another interesting choice as the preferred entry point is the upper bound of the allowed merging interval ($y_{\max}$). In general, this will require two turns, but will provide the minimum-time path to the point of exit from the merging interval, which could be of interest for reducing delays. These two choices are depicted in Fig. 13.

If the cost for the initial guess is strictly positive, which means that at least one of the constraints (whether it be entry interval or separation) is not satisfied, an iterative search for a minimizer is initiated. At each step k, a neighbor of the current $\delta^{(k)}$ is generated. This is done by randomly choosing an aircraft i and randomly incrementing or decrementing $\delta_i^{(k)}$ by a certain step size. The cost is then reevaluated, and a decision is made whether to move to this new point or not. This decision is the result of a random experiment [11]. The iterative process stops as soon as a point δ^* with negative cost $C(\delta^*)$ is found. Flexibility lies in the definition of the neighbor-generating function. Indeed, it can be tailored to provide certain characteristics of the updated δ, thereby guaranteeing certain properties of the overall solution. For example, the directions of the turns can be limited to a certain sign as a function of the x–y position of the aircraft, to ensure individual minimum-turn optimality of the solution. Another possible choice would be not to allow a certain subset of aircraft to maneuver away from the default trajectory.

Unlike gradient descent methods that may converge to a local minimum, simulated annealing has the ability to bypass these local minima and possibly find the global optimal. This fact is a result of the randomness, at each step, of the decision whether to move to the generated neighbor or not, even when this neighbor provides a worse cost than the previous point. This is crucial in the present problem, since a local minimum of the function C may not be negative. This would imply that no merging solution exists, while in fact an undetected negative global minimum may exist. This could arise, for instance, when a particular order of the aircraft after the merge cannot lead to a conflict-free solution. To change the order of the aircraft and find a suitable one, searching for neighbors that increase the cost C may be necessary.

If given enough time, the simulated annealing search will be able to handle these cases. However, in real-time applications, it is preferable to limit the time of the search. Whenever a search with a given initial guess finds no solution within several search iterations, alternate initial guesses that correspond to different ordering of the aircraft are provided. One way to obtain all possible orders feasible from a given aircraft configuration is to look at all possible combinations of initial turn durations, where each aircraft can either aim to merge at $y_{\min}$ or at $y_{\max}$. Indeed, a merging A/C will reach the exit point $(0, y_{\max})$ in minimum time by entering the target flow at $y_{\max}$ and in maximum time by entering at $y_{\min}$. There are 2^N such initial guesses. Therefore, performing parallel searches for all the initial guesses will become impractical when N is large. A sequential trial of the different initial points for the search until a solution is found is suggested.

B. Extension to Multiparameter Trajectories

In the previous discussion, the trajectory of each aircraft was characterized by a single parameter δ_i: namely, the duration of the first turn. This parameter completely described the turn-straight-turn merging trajectory, as it was assumed that the turns were performed at extreme turn rates and that the first turn was initiated at time t_0. The length of the straight segment and the final turn are determined by the requirement of effective merging onto the target flow. The solution to the conflict-free merging problem was obtained through an optimization scheme with respect to these N parameters δ_i.

The proposed method can easily be extended to solutions constructed from individual trajectories that can be parameterized by more than one parameter. For example, a second parameter for each aircraft can be introduced, representing the delay between time t_0 and the initiation of the first turn. With a nonzero value for this parameter, the resulting trajectory will be a straight segment in the direction of the initial heading, then a turn at full turn rate (for a duration equal to the value of the first parameter), followed by another straight segment and finally a turn into the target flow. Trajectories of this form are no longer Dubins paths. Therefore, no claim about time minimality can be made. However, as shown in Sec. II, if the turns are all in the same direction, then optimality with respect to the minimum-turn cost can be claimed.

With more parameters to describe the individual trajectories, more complex solutions can be obtained. Therefore, increasing the number of parameters over which the optimization is performed may provide solutions to a greater number of merging problems. For instance, for certain initial conditions the set of single-parameter trajectories may not be large enough to solve the problem, while the addition of extra parameters could provide a solution. An example of such an occurrence is given in the next section. Increasing the complexity of the parameterization of the trajectories does come at a cost. Indeed, the dimension of the search space for the simulated annealing

increases with the number of parameters. This leads to an increase in the search time and reduces the probability that the search will reach an existing solution in a reasonable time.

If no solution to this static optimization is found (i.e., there are no sets of aircraft trajectories that lead to a conflict-free merging) an alternate logic needs to be used. For instance, initiating the maneuvering earlier, or diverting certain A/C to a holding pattern or to another target flow could be considered. Avoiding these occurrences altogether is clearly a preferable alternative. This can be achieved by restricting the initial configurations to a feasible airspace, as investigated in Sec. V.

IV. Examples

In this section the performance of the proposed algorithm for several initial configurations of merging aircraft is demonstrated. At different times along the trajectories, the safety zones, which are circles of radius $\text{sep}_{\min}/2$ are plotted around the A/C positions, to illustrate that the minimum separation is met throughout the merging process. For each aircraft, the first circle marks the location of the A/C when the merging solution search is initiated. The upper and lower bounds on the merging points are delimited by horizontal dotted lines. The units are nautical miles, the minimum separation is 5 n mile, and the speed is $v = 8$ n mile/ min. The maximum turn rate is $u_{\max} = \pi$ rad/ min (2 min turn), leading to a minimum turn radius of 2.5 n mile. In some examples, as indicated in the text, a maximum turn rate of $u_{\max} = \pi/2$ rad/ min (4 min turn) and thus a minimum turn radius of 5 n mile are used.

In the first example, illustrated in Fig. 14, the preferred trajectory for each aircraft is the minimum-time path to the merging interval exit point $(0, y_{\max})$. As shown in Fig. 14a, if all aircraft follow their default paths, conflicts will occur (some circles representing the safety zones around the aircraft at some time intersect). Figure 14b shows the solution of the simulated annealing. Here, even though no constraint on the direction of first turn was added on the search space, the solution exhibits individual optimality with respect to minimum turn (see Sec. II).

In the second example, illustrated in Fig. 15, five aircraft merge in a person-by-person turn-optimal way. The maximum turn rate in this example is $u_{\max} = \pi/2$ rad/ min. Figure 15a shows the merging when no A/C maneuver away from their default trajectories, which in this example are the minimum-first-turn paths. This leads to separation constraint violations. Figure 15b depicts the merging solution. This example shows that a solution is found for a relatively congested airspace.

The third example, shown in Fig. 16, gives three possible solutions to a three-aircraft merge. The default trajectory is the minimum-first-turn trajectory (Fig. 16a). The solution depicted in Fig. 16b is individually optimal with respect to minimum turn, while those shown in Figs. 16c and 16d are not. Note that the solutions result in different ordering after the merge, so a preference in the order could motivate a certain choice.

In the example shown in Fig. 17, four A/C are merging into the target path. If the search for a conflict-free merging solution is restricted to the set of solutions where each aircraft trajectory is individually optimal, i.e., where the direction of the first turn is

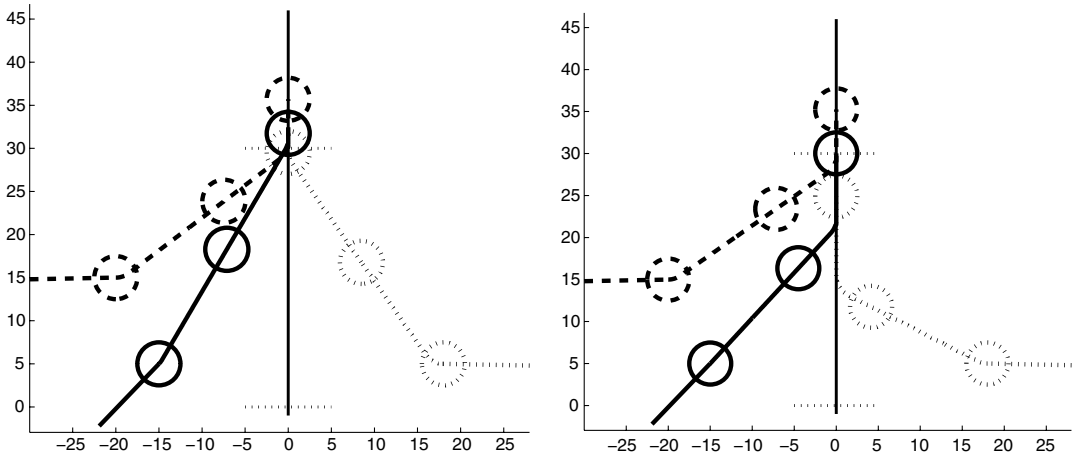

a) Default trajectories lead to separation loss **b) Conflict-free merging**

Fig. 14 Three-aircraft merge, with preference for minimum time to exit of merging interval.

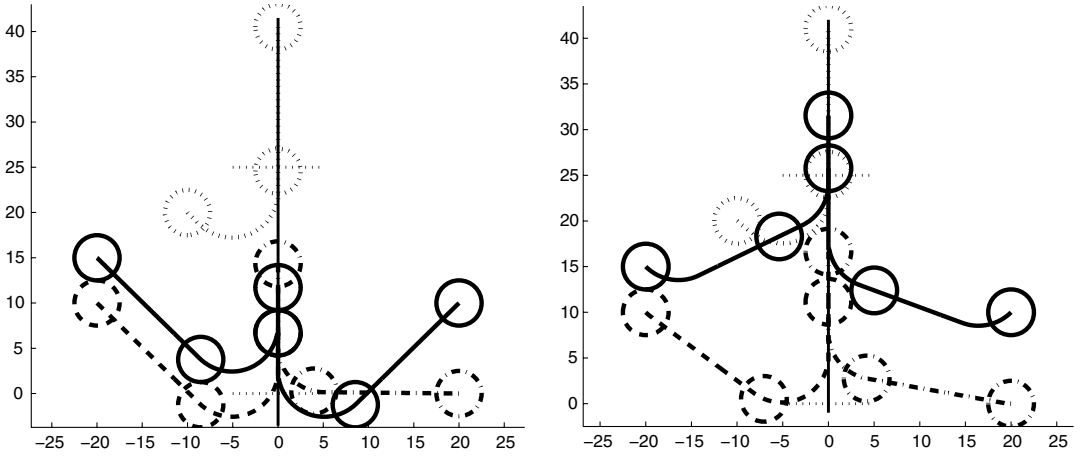

a) Default trajectories lead to separation loss **b) Conflict-free merging**

Fig. 15 Five aircraft merge, with preference for minimum initial turn.

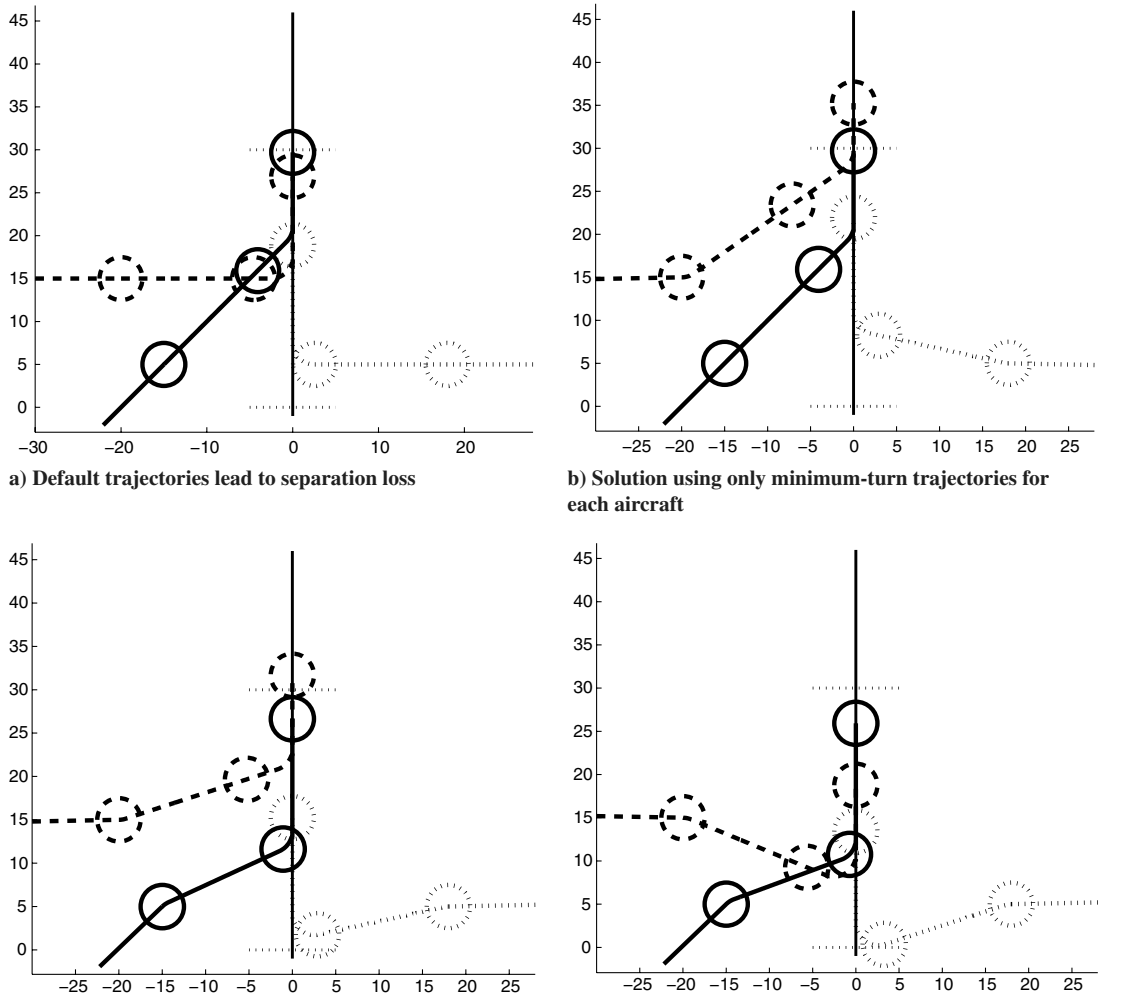

a) Default trajectories lead to separation loss

b) Solution using only minimum-turn trajectories for each aircraft

c) Solution when nonoptimal Dubin spath are allowed

d) Nonoptimal path can output a different order of the A/C

Fig. 16 Different solutions for a three-aircraft merge.

determined by the initial state of the aircraft, no solution is found. Figure 17b illustrates that a safe merging in this case will require some aircraft to enter the target path outside of the prescribed interval. It is worth noting that the sequencing that results from the algorithm is not straightforward. For example, in Fig. 17c the order after merging of the two A/C on the left might not have been an intuitive guess. It could be argued that the dashed-lined A/C on the left, though a bit further away from the y axis than the solid-lined A/C, would end up being the one ahead, since it is closer to the upper bound of the entry interval.

Finally, in the last example, depicted in Fig. 18, the trajectories are described by two parameters: the delay until the first turn and the duration of the first turn. The preferred trajectories are the minimum-time-to-exit paths and $u_{\max} = \pi/2\,\text{rad}/\,\text{min}$. With the initial configuration shown, the preferred trajectories lead to separation loss (see Fig. 18a). The case when no delay to first turn is allowed is illustrated in Figs. 18b and 18c. If only turn-optimal trajectories are allowed, the lower aircraft has very little maneuvering capability and no solution is found (Fig. 18b). A nonoptimal maneuver by this lower aircraft is required for a conflict-free merge (Fig. 18c). Allowing an initial delay before maneuvering provides a wider range of possible solutions. Figure 18d depicts a turn-optimal solution. The upper aircraft delays its initial turn until it passes behind the other aircraft, which does not maneuver away from the preferred trajectory.

The algorithm was tested on a personal computer running a quad-core processor with a clock speed of 2.6 Ghz. The computation time was recorded for sets of 100 randomly generated initial configurations. The average time, standard deviation, and maximum time for sets of simulations with increasing number of aircraft are summarized in Table 1. The data show that even with a basic computer used in this study, the computation times allow efficient real-time applications.

V. Statistical Study of Feasibility

In the above discussion and algorithm elaboration, it was assumed that all the aircraft could maneuver to provide a safe-merging solution. However, in practice, only a certain number of aircraft in the airspace (namely, those close to the target flow and merging interval) will be considered for merging and thus be inputs to the algorithm. To determine which aircraft in the airspace should be considered, a merging zone is defined: only aircraft within this zone are taken into account when making a decision regarding the required maneuvers for safe merging. For simplicity, a rectangular merging zone is assumed, characterized by two parameters: namely, the width and the height of the rectangle. The allowed entry interval is the portion of the target flow contained in the merging zone. This is illustrated in Fig. 19. The dimensions of the rectangle affect and in fact determine the existence of a safe-merging solution. The aim of the numerical, Monte-Carlo type study presented in this section is to better understand the relation between the design parameters, i.e., the merging zone dimensions, and the feasibility of a safe merge. This will also provide guidelines for choosing the merging zone parameters to ensure statistically the feasibility of effective merging solutions.

Based on the solution of an optimal control problem, a merging algorithm was derived, where the individual trajectories of the participating aircraft are constructed from two straight segments and two turns. In most cases, and especially for statistical analysis purposes, these turns can be assumed instantaneous and thus

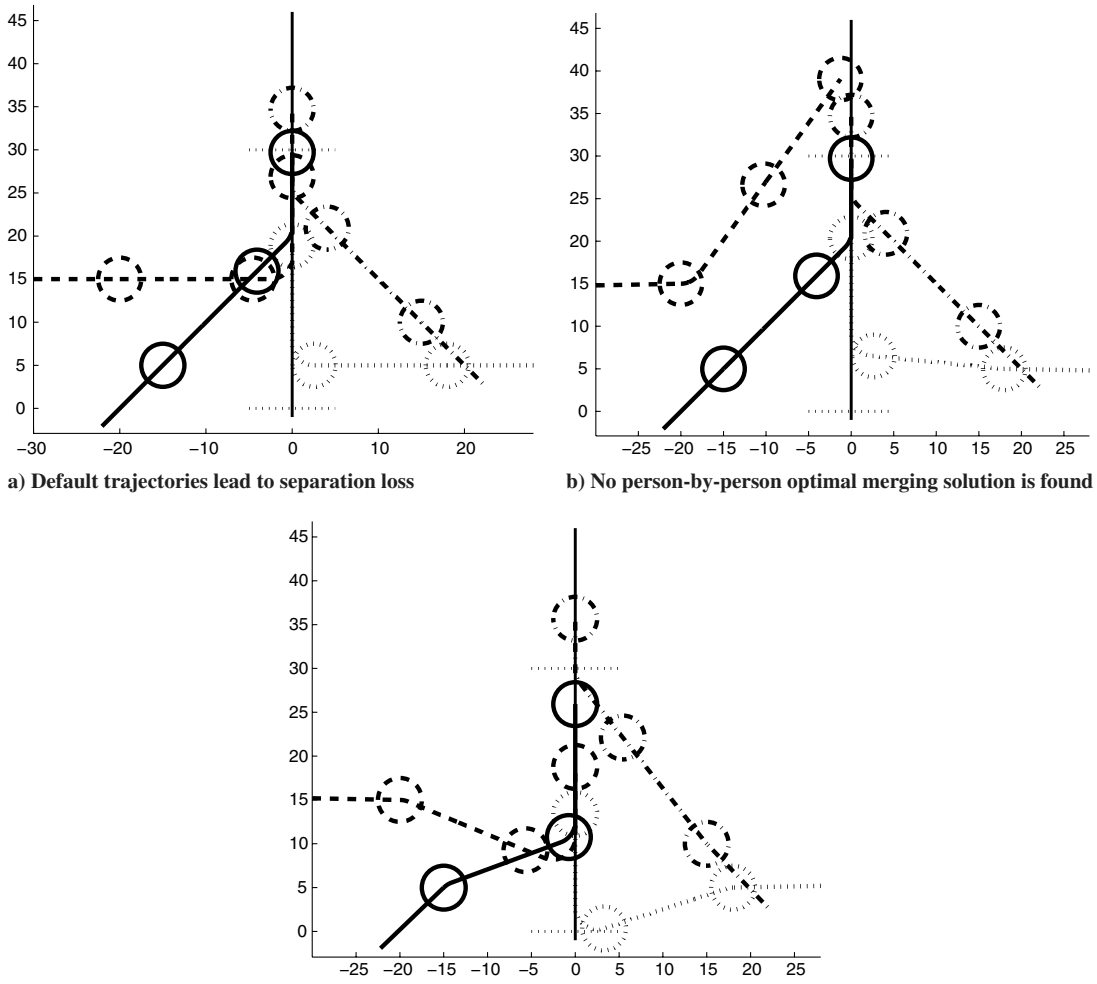

a) Default trajectories lead to separation loss

b) No person-by-person optimal merging solution is found

c) Conflict-free solution requires nonoptimal paths for some aircraft

Fig. 17 Four aircraft merge.

neglected. Consequently, the aircraft merging trajectories can be well approximated by two straight segments: one segment from the initial position to the final flow and one segment along the final flow until all aircraft have merged. With this approximation, a candidate merging solution is a set of N such two-segment trajectories, where N is the number of aircraft in the merging zone.

Let W be the half-width of the merging zone, and let L the length of the entry interval. In this study the minimum separation allowed $\text{sep}_{\min}$ is set to 5 n mile. The influence of these parameters on the success of the algorithm is investigated by having them vary within a certain range, and the output of the algorithm for all the possible values is observed. Values for W and L ranging from 5 to 25 n mile are examined. For each set of values (W_i, L_i) in the range, n_{runs} merging scenarios are generated and the empirical frequency of success of the algorithm is computed. This is done by randomly choosing an initial configuration for each run and checking if a safe approximate merging solution exists. The initial configuration is chosen according to a two-dimensional uniform distribution in the merging zone, with at least one aircraft on the left boundary of the box, to represent the choice of W.

The existence of a safe solution is determined in the following way. Given a set of positions for the aircraft involved in the merge, the entry interval is discretized, and all possible combinations of two-segment trajectories are inspected in a search for a solution where the minimum separation between the aircraft is ensured for the duration of the merge. If such a combination exists, the success count for that pair of parameter values is incremented by one. Given a number of A/C merging, the empirical probabilities of success give an idea of possible choices of dimensions for the merging zone, to provide an a priori probability that the algorithm will find a solution for merging the aircraft while maintaining minimum separation between the aircraft at all times.

Let A/C_1 and A/C_2 be a given pair of aircraft, with respective initial states $X1$ and $X2$ and initial velocity vectors $V1$ and $V2$ at time t_0. If their trajectories are approximated by two segments, one until the target flow is reached and one along the target flow, then the check for separation during the merge is simplified. Let $D_{t_0,X1,X2,V1,V2}(\tau)$ denote the distance at time τ between two points P1 and P2 traveling on a straight line, with positions and velocities of $(X1, V1)$ and $(X2, V2)$ at time t_0 (cf. Appendix B for the formula). Let T_1 and T_2 be the (approximate) times to reach the flow for A/C_1 and A/C_2, respectively. Without loss of generality, it is assumed here that $t_0 < T_1 < T_2$: i.e., that A/C_1 reaches the target flow before A/C_2.

1) When $t_0 < t < T_1$, A/C_1 travels on a straight line determined by $(X1, V1)$ and A/C_2 travels on a straight line determined by $(X2, V2)$. The minimum distance between the two aircraft during this time is with the previously defined notation:

$$D_{\min}^{1\text{st}_{\text{seg}}} = \min_{t_0 \le \tau \le T_1} D_{t_0,X1,X2,V1,V2}(\tau)$$

2) When $T_1 < t < T_2$, A/C_1 travels on the target flow, i.e., the y axis, and A/C_2 is still traveling on the straight line determined by $(X2, V2)$. The minimum distance between the two aircraft during this time is

$$D_{\min}^{2\text{nd}_{\text{seg}}} = \min_{T_1 \le \tau \le T_2} D_{T_1,X1(T_1),X2(T_1),\tilde{V}1,V2}(\tau) \quad \text{with} \quad \tilde{V}1 = \begin{bmatrix} 0 \\ v_1 \end{bmatrix}$$

Therefore, the minimal distance along the approximate default trajectories until both A/C have reached the flow is

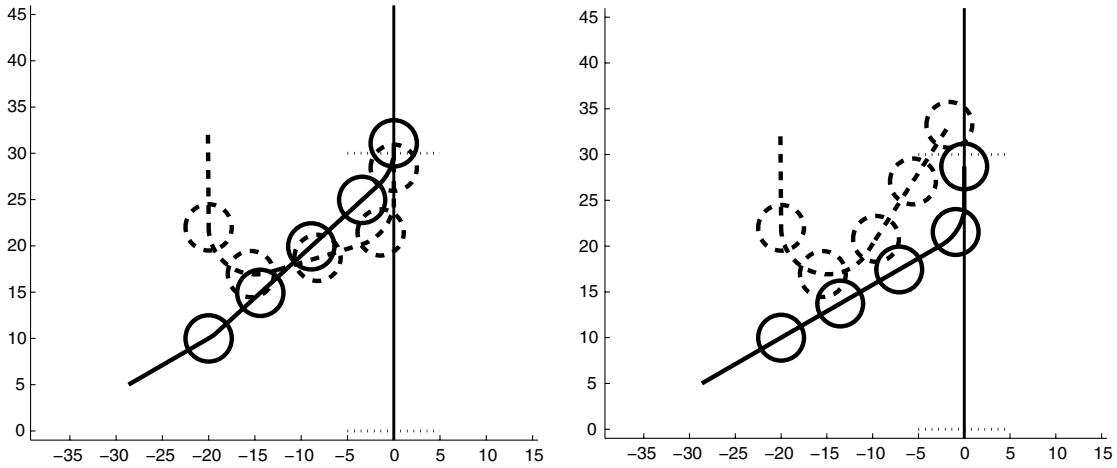

a) Default trajectories lead to separation loss

b) Only turn-optimal and zero-delay trajectories lead to conflict

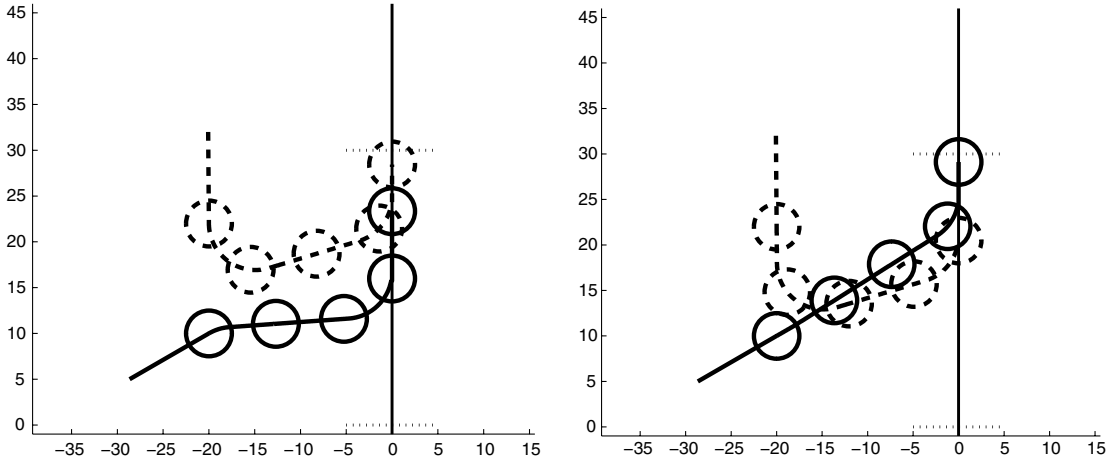

c) Nonoptimal and zero-delay provide a feasible solution

d) Turn-optimal solution, when delay can be nonzero

Fig. 18 More complex solutions may be required.

$$D^* = \min(D_{\min}^{1\text{st}_{\text{seg}}}, D_{\min}^{2\text{nd}_{\text{seg}}})$$

The empirical probabilities of success for the algorithm were generated for the $N = 2, 3.$ and 4 cases, by performing $n_{\text{runs}} = 1000$ per pair of values of the parameters W and L. The results are shown in Fig. 20. All three plots exhibit a certain level of symmetry with respect to the two variables W and L, which indicates that the influence of W and L are roughly identical. This means that improving chances of success can be almost equally achieved by increasing either one of the two parameters.

From Fig. 20a, it can be seen that for two merging A/C, when both W and L are equal to twice the minimum separation allowed, the algorithm has a very high probability ($\geq 95\%$) of success. The same level of frequency of success could be achieved with a lower value of one of the parameters at the expense of a higher value for the other. Figure 20b shows that for three A/C, if one looks at pairs of parameters with $W = L$, then a value of approximately three times the minimum separation for W and L is needed to attain a 95% success rate. Likewise, Fig. 20c shows that for four A/C, the same level of success requires W and L nearly four times the minimum separation. So choosing W and L to be equal to the minimum separation multiplied by the number of aircraft could be used as a rule of thumb for the design of the merging zone and provides a high a priori rate of success.

Table 1 Computation times

No. of A/C	Mean, s	Std dev	Max, s
3	0.81	1.65	7.70
4	1.54	2.39	8.93
5	3.74	4.29	17.10
6	7.04	5.98	22.67

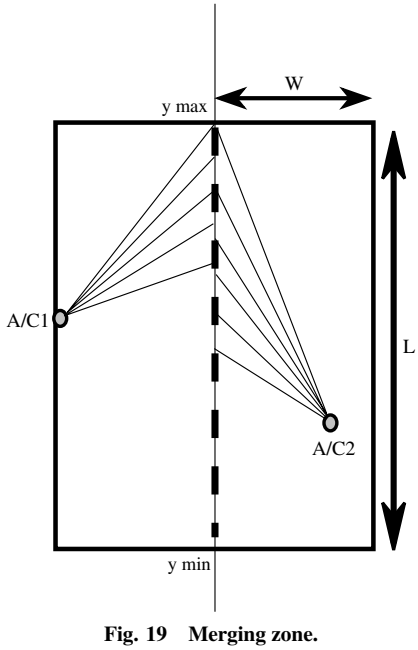

Fig. 19 Merging zone.

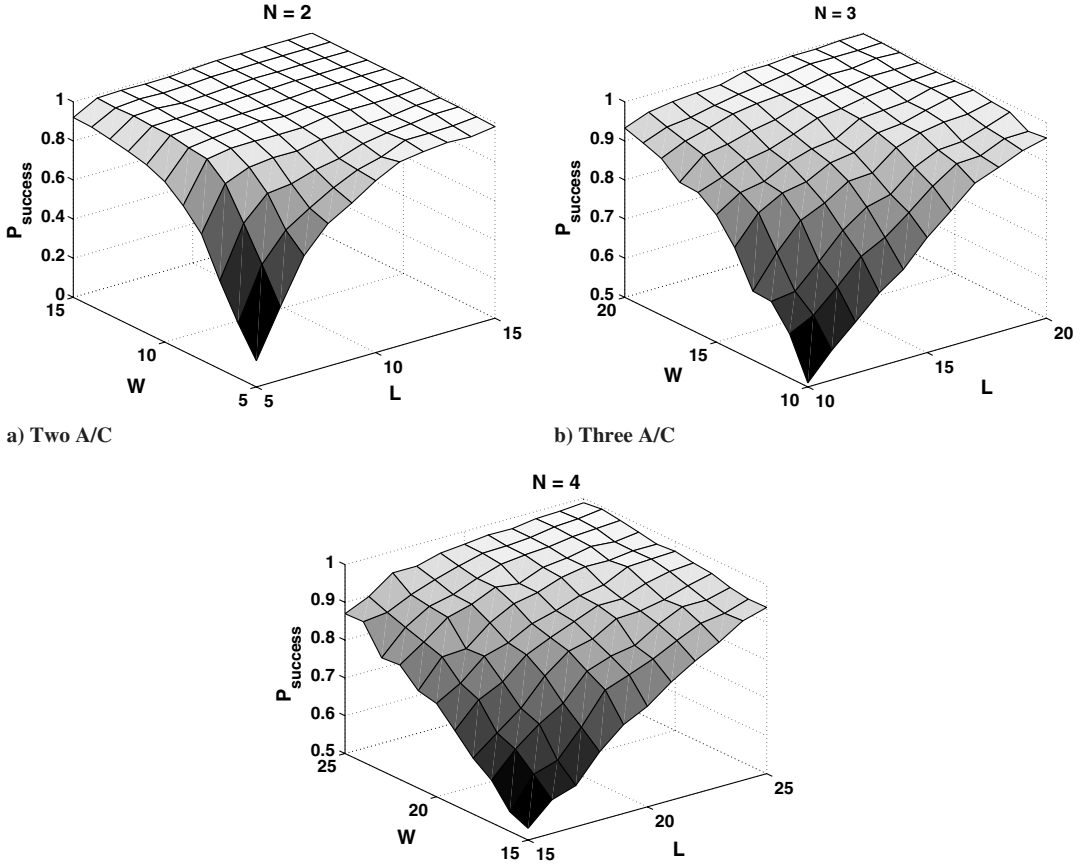

a) Two A/C

b) Three A/C

c) Four A/C

Fig. 20 Empirical probabilities of success.

According to the same plots, a 99% a priori success probability is achieved when W and L are both equal to 15 n mile for the two-A/C case, 20 n mile for the three-A/C case, and 25 n mile for the four-A/C case. The intuition that a greater number of A/C merging will require a larger maneuvering zone to attain a certain level of probability of success is supported by the three plots in Fig. 20. Also note that since the instantaneous-turn assumption is made to construct these empirical probabilities, and since this assumption's validity is stronger for larger scales, the probabilities are more realistic when W and L are large.

It should be noted that these empirical distributions do not take any airspace structure into account. Therefore, for a given number of A/C, all possible configurations within the zone are equally considered when computing the empirical frequencies. This is clearly neither realistic nor optimal. Indeed, randomly chosen initial configurations that lead to a failure of the algorithm but do not arise in practice in fact artificially lower the empirical rate of success. Therefore, these distributions provide upper bounds on the required values of the parameters for a desired success probability. If a particular structure of the airspace (i.e., the geometry of the incoming flows with respect to the target flow) is known or specified, this information can be exploited in the analysis and design of the merging zone. Typically, if the structure of the incoming flows is limited to a certain geometry, in most cases it will be possible to choose values for W and L lower than those obtained from the plots in Fig. 20, since the merging zone has to be tailored only to these particular flows.

VI. Conclusions

An algorithm for the horizontal merging of multiple aircraft into a flow was presented. It is based on minimum-turn trajectories of a single aircraft merging onto the target flow. The aircraft are assumed to merge into a given interval along the flow without specifying a particular entry point along this interval. The aircraft merging sequence is assumed to be unknown and is obtained as part of the solution. The solutions to this problem were derived from Pontryagin's maximum principle. Exact global solutions for a single A/C were obtained for any initial state. It was shown that there may be an infinite number of optimal trajectories, which is an interesting aspect of the problem. With multiple aircraft merging, the requirement that minimum separation between any two aircraft be maintained at all times is added. The algorithm generates a set of trajectories for every aircraft, by deviating from the single aircraft optimal path. By constraining the set of deviations, the optimality of each individual trajectory can be enforced. For some initial configurations of aircraft there may not exist a solution to the safe-merging problem. This would usually result from initiating the solution at an aircraft configuration that is too close to the target flow. In this case, one would have to restart the search at an earlier time to increase the solution probability through an increase in the aircraft maneuver space. A statistical study was carried out to provide a priori empirical probabilities of success for different choices of problem parameters. The proposed methodology could provide a realistic solution for a large number of merging aircraft in a real-time setting.

Acknowledgment

This work was partially supported by NASA Ames Research Center grant NNA06CN22A.

Appendix A: Nonoptimality of Multiple-Alternating-Turn Trajectories

In Sec. II, first-order necessary conditions for minimum-turn trajectories were derived. These led to two possible fundamental structures for the solutions: either the solution was the result of turns in only one same direction (including zero turn) from initial to final

time, or there existed two parallel switch lines. Between these lines the turn rate was zero, and outside of the lines the turn rate was extremal in the two opposite directions on each side of the lines. So S-shaped trajectories satisfy the first-order conditions for optimality. Trajectories with multiple alternating turns with straight segments between the turns, as depicted in Fig. A1 also satisfy the first-order necessary conditions. However, such trajectories are never turn-optimal. Figure A1 is the graphical proof of this fact.

The idea of the proof is the following. Consider the most general case of multiple-alternating-turn trajectories, as shown in Fig. A1. For all possible cases of initial and final points along this trajectory, which require strictly more than two alternate turns, another path is constructed, which has a lower cost in terms of total amount of turning. The circles shown are of radius $v/u_{\max}$: i.e., the aircraft turns at extreme turn rate along these circles. The dashed lines are the switch lines introduced in Sec. II. In the following discussion, point B will be called downstream from point A if an aircraft travels along the trajectory from A to B in the same direction as the arrow. Equivalently, point A will be said to be upstream from point B. Also, note that a point of the trajectory is characterized by its position and its velocity vector (or heading).

First, it is assumed that the initial point is on the arc AB (B excluded) of the figure. Let the terminal point G be any point on the straight segment DE immediately downstream from D, as shown in Fig. A2. Let F be the point on the arc AB such that leaving from F, a straight segment followed by an extreme turn arrives exactly at G. If the initial point X_0 is anywhere upstream from F, then the path X_0-F-G clearly has a lower cost than X_0-B-C-D-G, since the first and second turns are both shorter for the first path. If X_0 is on the FB arc, point B excluded, then making no initial turn, going straight, turning at extreme rate into the segment DG (upstream of G) and then going straight to G is also a lower-cost path than X_0-B-C-D-G. This shows that for any point G of segment DE and any initial point X_0 of arc AB, B excluded, there exists a lower-cost path than the original path. Therefore, the path X_0-B-C-D-G cannot be optimal for any G on DE

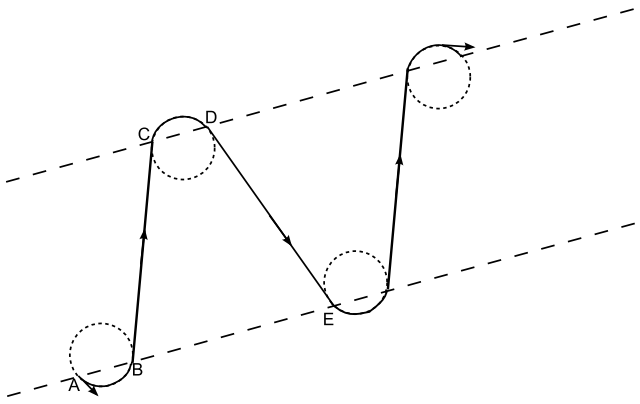

Fig. A1 General multiple-alternating-turn trajectory.

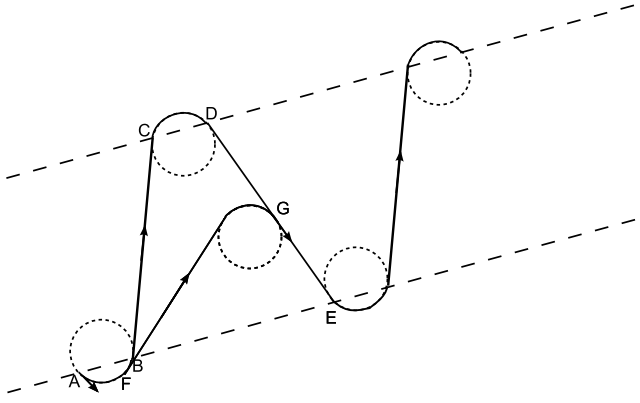

Fig. A2 Lower-cost path from A to G.

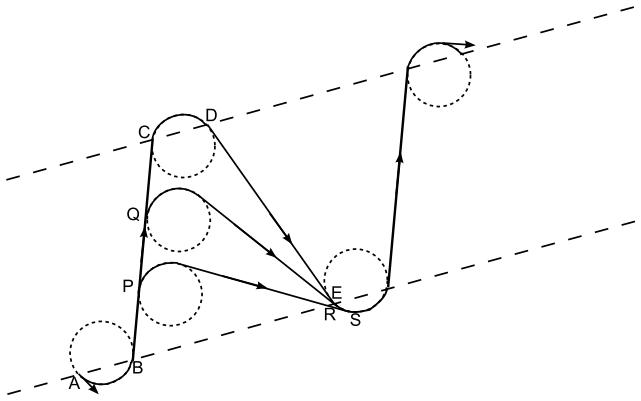

Fig. A3 Lower-cost paths from P to R and S.

(and, by immediate implication, for all points downstream of G). Since the point G was fixed arbitrarily, the conclusion holds for all points strictly downstream of D.

Another possibility is for the initial point to be on the segment BC. Let P and Q be two points of segment BC depicted in Fig. A3, and let S (respectively, R) be the point on the arc immediately downstream from point E, such that a point leaving from P (respectively, Q) at extreme rate, then going straight, will arrive tangentially to the circle going through E. Now assume that the initial point is at P. If the terminal point is at S, then the path P-S has clearly a lower cost than the path P-C-D-S, since the first and second turns are both shorter for the first path. It immediately follows that this is also true for any terminal point downstream from S. If the terminal point is at R, then the path P-Q-R has a lower cost than P-C-D-R, for the same reason as the previous case. Such a point Q exists for any point R on the arc ES. So it has been shown that for any point P on the segment BC and for any terminal points on arc ES or downstream of S, there exists a path of lower cost than the original trajectory. Therefore, for any initial point on segment BC and terminal point strictly downstream of point E, the suggested trajectory is nonoptimal.

So to summarize, the following have been shown by construction:

1) If the initial point is on a turn, the depicted trajectory will never be optimal for any terminal point on the trajectory strictly downstream of the end of the second turn portion.

2) If the initial point is on a straight portion of the trajectory, the depicted trajectory will never be optimal for any terminal point strictly downstream of the end of the second straight portion.

This in fact proves that trajectories with turns in alternating directions can have two turns at most and that these two turns are necessarily at the beginning and end of the trajectory in this case. If the trajectory starts or ends with a straight segment, then it can only have a turn in one direction for it to be optimal.

Appendix B: Minimum Distance Along Segments

Consider the following problem: given two points $X1$ and $X2$ traveling along straight lines in $\mathbb{R}^2$ at respective speeds v_1 and v_2, what is the minimum distance D between them during a specified interval of time $[a, b]$?

The dynamics in vector form are $\mathbf{X}i(t) = \mathbf{X}i(t_0) + (t - t_0)\mathbf{V}i$ for $i = 1, 2$. In x–y space,

$$\mathbf{X}\,i = \begin{bmatrix} x_i \\ y_i \end{bmatrix}$$

and

$$\mathbf{V}\,i = \begin{bmatrix} v_i \cos(\theta_i) \\ v_i \sin(\theta_i) \end{bmatrix}$$

is a constant-direction vector for line i.

Let $\Delta\mathbf{X}(t) = \mathbf{X}1(t) - \mathbf{X}2(t)$ and $\Delta\mathbf{V}(t) = \mathbf{V}1(t) - \mathbf{V}2(t)$. Hence, the problem is to determine

$$D(t^*) = \min_{t\in[a,b]} D(t) = \min_{t\in[a,b]} \|\Delta\mathbf{X}(t)\|$$

First, note that t^* minimizing $D(t)$ also minimizes $D^2(t)$, since $D > 0$ and the square function is increasing on $\mathbb{R}^+$. So,

$$\frac{\mathrm{d}}{\mathrm{d}t} D^2(t) = \frac{\mathrm{d}}{\mathrm{d}t} \|\Delta\mathbf{X}(t)\|^2 = 2 < \frac{\mathrm{d}}{\mathrm{d}t}\Delta\mathbf{X}, \Delta\mathbf{X} > = 2\langle \Delta\mathbf{V}, \Delta\mathbf{X}\rangle$$

and

$$\begin{aligned}
&\frac{\mathrm{d}}{\mathrm{d}t} D^2(t) = 0 \qquad \Leftrightarrow \langle \Delta\mathbf{V}, \Delta\mathbf{X}\rangle = 0 \\
&\Leftrightarrow \langle \Delta\mathbf{V}, \Delta\mathbf{X}(t_0) + (t - t_0)\Delta\mathbf{V}\rangle = 0 \\
&\Leftrightarrow \langle \Delta\mathbf{V}, \Delta\mathbf{X}(t_0)\rangle + (t - t_0)\|\Delta\mathbf{V}\|^2 = 0
\end{aligned}$$

If $\Delta\mathbf{V} = 0$, then D^2 is constant on $[a, b]$, and so is D:

$$D^* = \|\Delta\mathbf{X}(t_0)\|$$

If $\Delta\mathbf{V} \neq 0$, the minimum along the lines is reached at time

$$\hat{t} = t_0 - \frac{\langle \Delta\mathbf{V}, \Delta\mathbf{X}(t_0)\rangle}{\|\Delta\mathbf{V}\|^2}$$

Since $\hat{t}$ might be outside the interval $[a, b]$, and since the D^2 is a square function of t with positive coefficient, one gets

$$t^* = \begin{cases} a & \text{if } \hat{t} < a \\ \hat{t} & \text{if } a \le \hat{t} \le b \\ b & \text{if } \hat{t} > b \end{cases}$$

Once t^* is known,

$$D^{*2} = D^2(t^*) = \|\Delta\mathbf{X}(t_0) + (t^* - t_0)\Delta\mathbf{V}\|^2$$

An interesting special case is when $a = t_0$ and $\Delta\mathbf{V} \neq 0$. Then

$$t^* = \begin{cases} t_0 & \text{if } \hat{t} < t_0 \\ \hat{t} & \text{if } t_0 \le \hat{t} \le b \\ b & \text{if } \hat{t} > b \end{cases}$$

which gives

$$t^* - t_0 = \begin{cases} 0 & \text{if } -\frac{\langle \Delta\mathbf{V}, \Delta\mathbf{X}(t_0)\rangle}{\|\Delta\mathbf{V}\|^2} < 0 \\ -\frac{\langle \Delta\mathbf{V}, \Delta\mathbf{X}(t_0)\rangle}{\|\Delta\mathbf{V}\|^2} & \text{if } 0 \le -\frac{\langle \Delta\mathbf{V}, \Delta\mathbf{X}(t_0)\rangle}{\|\Delta\mathbf{V}\|^2} \le b - t_0 \\ b - t_0 & \text{if } -\frac{\langle \Delta\mathbf{V}, \Delta\mathbf{X}(t_0)\rangle}{\|\Delta\mathbf{V}\|^2} > b - t_0 \end{cases}$$

Since

$$\begin{aligned}
D^{*2} &= \|\Delta\mathbf{X}(t_0) + (t^* - t_0)\Delta\mathbf{V}\|^2 = \|\Delta\mathbf{X}(t_0)\|^2 \\
&\quad + \|(t^* - t_0)\Delta\mathbf{V}\|^2 + 2\langle \Delta\mathbf{X}(t_0), (t^* - t_0)\Delta\mathbf{V}\rangle
\end{aligned}$$

when

$$t^* - t_0 = -\frac{\langle \Delta\mathbf{V}, \Delta\mathbf{X}(t_0)\rangle}{\|\Delta\mathbf{V}\|^2}$$

$$\begin{aligned}
D^{*2} &= \|\Delta\mathbf{X}(t_0)\|^2 + (t^* - t_0)^2\|\Delta\mathbf{V}\|^2 + 2(t^* - t_0)\langle \Delta\mathbf{X}(t_0), \Delta\mathbf{V}\rangle \\
&= \|\Delta\mathbf{X}(t_0)\|^2 + \frac{\langle \Delta\mathbf{V}, \Delta\mathbf{X}(t_0)\rangle^2}{\|\Delta\mathbf{V}\|^2} - 2\frac{\langle \Delta\mathbf{V}, \Delta\mathbf{X}(t_0)\rangle^2}{\|\Delta\mathbf{V}\|^2} \\
&= \|\Delta\mathbf{X}(t_0)\|^2 - \frac{\langle \Delta\mathbf{V}, \Delta\mathbf{X}(t_0)\rangle^2}{\|\Delta\mathbf{V}\|^2} \\
&= \|\Delta\mathbf{X}(t_0)\|^2[1 - \cos^2(\angle(\Delta\mathbf{V}, \Delta\mathbf{X}(t_0)))]
\end{aligned}$$

So, finally, in this case,

$$D^* = \|\Delta\mathbf{X}(t_0)\|\sqrt{[1 - \cos^2(\angle(\Delta\mathbf{V}, \Delta\mathbf{X}(t_0)))]}$$

References

[1] "Capacity Needs in the National Airspace System, 2007-2025," Federal Aviation Administration, 2007.

[2] "Terminal Area Forecast Summary, Fiscal Years 2007–2025, Federal Aviation Administration, 2007.

[3] Davis, T. J., Krzeczowski, K. J., and Bergh, C., "The Final Approach Spacing Tool," *13th IFAC Symposium on Automatic Control in Aerospace*, Sept. 1994.

[4] Robinson, J. E., III, Davis, T. J., and Isaacson, D. R., "Fuzzy-Reasoning-Based Sequencing of Arrival Aircraft in the Terminal Area," AIAA Guidance, Navigation, and Control Conf., AIAA Paper 1997-3542, Aug. 1997.

[5] Robinson, J. E., III, and Isaacson, D. R., "A Concurrent Sequencing and Deconfliction Algorithm for Terminal Area Air Traffic Control," AIAA Guidance, Navigation, and Control Conf., AIAA Paper 2000-4473, Aug. 2000.

[6] Erzberger, H., and Lee, H. Q., "Optimal Horizontal Guidance Techniques for Aircraft," *Journal of Aircraft*, Vol. 8, No. 2, 1971, pp. 95–101. doi:10.2514/3.44235

[7] Pecsvaradi, T., "Optimal Horizontal Guidance Law for Aircraft in the Terminal Area," *IEEE Transactions on Automatic Control*, Vol. 17, No. 6, Dec. 1972, pp. 763–772. doi:10.1109/TAC.1972.1100160

[8] Bolender, M., and Slater, G. L., "Departure Trajectory Synthesis and the Intercept Problem," AIAA Guidance, Navigation, and Control Conf., AIAA Paper 1997-3545, Aug. 1997.

[9] Krozel, J., Capozzi, B., Andre, A. D., and Smith, P., "The Future National Airspace System: Design Requirements Imposed By Weather Constraints," AIAA Guidance, Navigation, and Control Conf., AIAA Paper 2003-5769, 2003.

[10] Niedringhaus, W. P., "Stream Option Manager (SOM): Automated Integration of Aircraft Separation, Merging, Stream Management, and Other Air Traffic Control Functions," *IEEE Transactions on Systems, Man, and Cybernetics*, Vol. 25, No. 9, Sept. 1995, pp. 1269–1280. doi:10.1109/21.400505

[11] Kirkpatrick, S., Gelatt, C. D., and Vecchi, M. P., "Optimization by Simulated Annealing," *Science*, New Series, Vol. 220, No. 4598, 1983, pp. 671–680. doi:10.1126/science.220.4598.671

[12] Bryson, A., and Ho, Y. C., *Applied Optimal Control*, Taylor & Francis, New York, 1975, pp. 47–89, chap. 2.

[13] Pontryagin, L. S., *The Mathematical Theory of Optimal Processes*, Wiley, New York, 1962, pp. 9–114, Chaps. 1–2.

[14] Dubins, L. E., "On Curves of Minimal Length with a Constraint on Average Curvature, and with Prescribed Initial and Terminal Positions and Tangents," *American Journal of Mathematics*, Vol. 79, No. 3, 1957, pp. 497–516. doi:10.2307/2372560

[15] Boissonnat, J-D., Cerezo, A., and Leblond, J., "Shortest Paths of Bounded Curvature in the Plane," *Journal of Intelligent and Robotic Systems: Theory and Applications*, Vol. 11, Nos. 1–2, 1994, pp. 5–20. doi:10.1007/BF01258291